Characterization of Saturated Hydrocarbons in Vacuum Petroleum Residua: Redox Derivatization Followed by Negative-Ion Electrospray Ionization Fourier Transform Ion Cyclotron Resona...

ARTICLE *in* ENERGY & FUELS · DECEMBER 2013

Impact Factor: 2.79 · DOI: 10.1021/ef4016284

energy&fuels

Article

pubs.acs.org/EF

Characterization of Saturated Hydrocarbons in Vacuum Petroleum Residua: Redox Derivatization Followed by Negative-Ion Electrospray Ionization Fourier Transform Ion Cyclotron Resonance Mass Spectrometry

Xibin Zhou,[†,‡] Yahe Zhang,[†] Suoqi Zhao,[†] Keng H. Chung,[†,§] Chunming Xu,[†] and Quan Shi*[,†]

[†]State Key Laboratory of Heavy Oil Processing, China University of Petroleum, Beijing 102249, People's Republic of China

[‡]College of Pharmacy, Liaoning Medical University, Jinzhou, Liaoning 121000, People's Republic of China

[§]Well Resources Incorporated, 3919-149A Street, Edmonton, Alberta T6R 1J8, Canada

ABSTRACT: Heavy petroleum fractions, which have distinct chemical and physical properties, are becoming important refinery feedstocks. In comparison to aromatic and heteroatom-containing compounds, the saturate compounds in heavy petroleum fractions have rarely been analyzed using recent advanced mass spectrometry methods. In this work, the compositions of saturate fractions derived from six vacuum residua (VR) of different geological origins were determined and compared. Saturate fractions were subjected to ruthenium-ion-catalyzed oxidation (RICO) derivatization and characterized with negative-ion electrospray ionization (ESI) Fourier transform ion cyclotron resonance mass spectrometry (FT-ICR MS). The results showed that the VR-derived saturates consisted of *n*-paraffins, isoparaffins, and naphthenes with 1−10 rings. The maximum double bond equivalent (DBE) values of species in various VR-derived saturates were similar. The maximum carbon number of VR-derived saturates was up to 100. The maximum carbon numbers of naphthenes in VR-derived saturates were generally greater than that of paraffins. The relative abundances and ranges of carbon numbers of the various species in VR-derived saturates differed depending upon their geological origin and the distillation temperature of samples. Compounds with 0−6 naphthenic rings were highly abundant in the VR-derived saturates. On the basis of the results of this study, the RICO/ESI FT-ICR MS method shows promise as a potential semi-quantitative analysis for saturates in heavy petroleum fractions.

INTRODUCTION

Saturated hydrocarbons are major components of petroleum feedstock. Having a better understanding of the nature of saturated hydrocarbons in petroleum-derived streams will allow the refineries to optimize refining processes. The saturated hydrocarbons in distillate fractions have been extensively investigated.[1−3] However, the molecular composition of saturated hydrocarbons in vacuum residua (VR) is not well-understood, because of the lack of appropriate analytical tools to characterize high-boiling-point hydrocarbons.

Various analytical techniques, such as multi-dimensional gas chromatography (GC) and high-resolution mass spectrometry (MS) have been used to analyze heavy petroleum fractions. High-resolution Fourier transform ion cyclotron resonance (FT-ICR) MS has been the only technique capable of fully analyzing highly complex molecules in heavy petroleum fractions. Schaub et al. and Smith et al.[4,5] used an automated liquid injection field desorption (LIFD) ionization coupled with FT-ICR MS for nonpolar species analysis and found that automated LIFD facilitates averaging of hundreds of mass spectra for increased dynamic range, mass accuracy, and signal-to-noise (S/N) ratio relative to single-application field desorption experiments. However, no follow-up studies were reported. Wu et al.[6] reported that saturates can be oxidized *in situ* by initiating an electrical discharge during desorption electrospray ionization (DESI). With betaine aldehyde incorporating spray, it enables the rapid and direct analysis of alkanes at atmospheric pressure without sample preparation. The technique was successfully implemented for analysis of petroleum distillates containing saturated hydrocarbons. However, the poor selectivity of the process to produce solely mono-oxidized products restricted it for a routine approach for saturate characterization. Other ionization techniques commonly used in FT-ICR MS, such as electrospray ionization (ESI), atmospheric pressure photoionization (APPI), and atmospheric pressure chemical ionization (APCI), are able to ionize many saturates, but the ionization efficiency for linear paraffins is low and limited by a large matrix effect.[7]

Chemical ionization (CI) provides soft ionization of saturated hydrocarbons[8−10] and polyethylene.[11−14] Campbell et al.[15,16] and Duan et al.[17,18] used the laser-induced acoustic desorption (LIAD) CI MS under vacuum coupled with the use of a cyclopentadienyl cobalt radical cation or ligated water cluster of Mn^+ $[ClMn(H_2O)^+]$ for analyzing saturated hydrocarbons. Large molecules and highly branched saturates can be vaporized and routed to the mass spectrometer without fragmentation. Nyadong et al.[19] used LIAD with O_2 as a carrier/reagent gas to analyze saturated hydrocarbons. In this method, the straight-chain, branched, and cycloalkanes could be ionized with minimum or no fragmentations. The $[M - H]^+$ ions were dominant species for straight-chain and branched alkanes. For cycloalkanes, M^+ species were dominant on the

Received: June 28, 2013
Revised: December 3, 2013
Published: December 13, 2013

mass spectrum at low capillary temperatures (<100 °C) and $[M - H]^+$ species were dominant on the mass spectrum at high capillary temperatures (>200 °C). This CI method can be operated under atmospheric pressure and easily coupled with FT-ICR MS.

Recently, Zhou et al.[20] developed a chemical derivatization method for analyzing saturates in heavy petroleum fractions using ESI FT-ICR MS. A ruthenium-ion-catalyzed oxidation (RICO) reaction was used to transform saturates into alcohols, which could be ionized by ESI. Branched paraffins and naphthenes with tertiary C−H bonds were oxidized to alcohols, which could be ionized by negative-ion ESI. The *n*-paraffins without tertiary C−H bonds were converted to ketones, which could be reduced by $LiAlH_4$ to form alcohols. Hence, *n*-paraffins could be discriminated from isoparaffins. Because negative-ion ESI produces only the $[M - H]^-$ ions, the use of RICO derivatization followed by ESI results in a simplified mass spectrum and enables semi-quantitative analysis of heavy saturates. ESI also provides a continuous and stable ion stream, which allows for the co-added mass spectra acquisition for improved S/N ratio and detection dynamic range.

In this study, saturate hydrocarbons in six VR were subjected to RICO derivatization and characterized by negative-ion ESI FT-ICR MS. The objective of the research was to compare the molecular compositions of saturates as a function of the origin of petroleum crude.

EXPERIMENTAL SECTION

Materials. Six VR samples originating from various sources [China Liaohe (LS) and Tahe (TS), Venezuela (two samples, VS1 and VS2), Canada oil sands bitumen (CS), and Sudan (SS)] were used in this work. The LS and VS1 were obtained from a commercial vacuum distillation unit operated at 420 °C at the PetroChina Liaohe Petrochemical Company. The rest of the VR samples were 500 °C+ residues obtained from a laboratory vacuum distillation unit. The saturate fraction of each VR sample was obtained by saturate, aromatic, resin, and asphaltene (SARA) fractionation using the Chinese Standard Analytical Method for Petroleum and Natural Gas Industry: SH/T 0509-92, which is equivalent to ASTM D2007-93.

Chemical Derivation of Saturated Hydrocarbons. The saturates (30 mg) was mixed with a blend of 2 mL of tetrachloromethane (CCl_4), 2 mL of acetonitrile (CH_3CN), 3 mL of water, 0.25 g of sodium periodate ($NaIO_4$) (1.17 mmol), and 5 mg of ruthenium chloride ($RuCl_3$) in a 12 mL sealed sample vial. The mixture was continuously stirred with a small magnetic bar for 24 h at 40 °C. The organic and aqueous phases of the reaction product were collected. The aqueous phase was extracted with 1 mL of chloroform ($CHCl_3$) 3 times. The $CHCl_3$-derived organic extracts were combined and dried with sodium sulfate (Na_2SO_4). The organic extract was divided into two equal portions. Portion 1 was subjected to the potassium hydroxide (KOH)-modified silica gel chromatography using 20 mL of $CHCl_3$ as the eluent to remove the acids, which derived from alkylated aromatics in the saturate fraction.[21] The monohydric alcohols in the eluate were analyzed by negative-ion ESI FT-ICR MS for isoparaffins and naphthenes. Portion 2 was subjected to KOH-modified silica gel chromatography using 25 mL of a tetrahydrofuran (THF)/$CHCl_3$ (1:1, v/v) mixture as the eluent to remove the acids. The eluate was dried in a rotary evaporator. The acids-free eluate sample was subjected to reduction reactions with lithium aluminum hydride ($LiAlH_4$) (0.2 g, 5.27 mmol) in dry THF under reflux for 24 h. The $LiAlH_4$-reduced product was subjected to silica gel chromatography using 20 mL of $CHCl_3$ eluent to yield monohydric alcohols,[20] which were analyzed by negative-ion ESI FT-ICR MS for paraffins and naphthenes.

High-Temperature Gas Chromatography (HT-GC) Analysis. The HT-GC analysis was performed using AC Agilent 6890N high-temperature simulated distillation gas chromatography (AC, Netherlands). A total of 10 mg of the saturate fraction was dissolved in 800 mg of CS_2. 1 μL of sample was injected into a HT750 capillary column (5 m × 0.53 mm × 0.1 μm, from AC).

The GC oven temperature was programmed to increase from 40 to 430 °C at 10 °C/min and kept constant for 5 min once it reached 430 °C. The initial temperature of the injection port was 100 °C, which was increased to 430 °C at a rate of 15 °C/min, and then kept constant for 22 min. The detector was kept at 430 °C. The data acquisition frequency was 50 Hz.

ESI FT-ICR MS Analysis. The monohydric alcohol solution (0.1 mL) obtained from the chromatography was diluted with 1 mL of a toluene/methanol (1:3, vol/vol) mixture. To facilitate deprotonation of alcohols to yield $[M - H]^-$ ions, 20 μL of 25% NH_4OH was added to the final solution.

The MS analyses were conducted using Bruker apex-ultra 9.4 T FT-ICR MS equipped with ESI. The sample solution was introduced into the Apollo II electrospray source using a 250 μL syringe equipped with a syringe pump. The flow rate of sample was 180 μL/h. The conditions of ESI were as follows: 4 kV emitter voltage, 4.5 kV capillary column introduce voltage, and −320 V capillary column end voltage. Deprotonated analyte ions were collected through two-stage ion funnels, passed through a radio-frequency (RF) hexapole and a quadrupole mass analyzer (Q1), and then injected into a collision cell. The optimized mass for the quadrupole (Q1) was 200 Da. An argon-filled hexapole collision pool was operated at 5 MHz and 700 V_{p-p} of RF amplitude, and the ions accumulation time was 0.01−0.05 s. The optimized time-of-flight (ToF) for the ions extracted from the collision pool to the ICR cell was 1.8 ms, which provided a large signal intensity and broad mass range. The RF excitation of the ion cyclotron resonance cell was attenuated at 12 dB, and the sidekick was at −9.9 V. The sidekick offset was at 3 V. The mass range was set at m/z 154−2000. A total of 300 FT-ICR data scans with 4M word size were co-added to generate the mass spectra.

Mass Calibration and Data Analysis. The internal mass calibration was performed using a G2421A electrospray "tuning mix" acetonitrile solution from Agilent. After the acetonitrile solution sample was analyzed, the mass spectra were recalibrated using a known series of O_1 class species.

Data analysis was performed using Bruker data analysis (DA) software. Peaks with S/N greater than 5 were exported to a spreadsheet. The detailed data processing procedure has been described elsewhere.[22−24]

Hydrogen/Carbon (H/C) Ratio of Saturated Hydrocarbons by FT-ICR MS. The FT-ICR MS data were used to calculate the H/C ratios of saturate fractions. The H/C ratio is shown in eq 1

$$\mathrm{H/C} = \frac{\sum nH_i I_i}{\sum nC_i I_i} \quad (1)$$

where nH_i is the hydrogen number, I_i is the peak height of each defined O_1 component, and nC_i is the carbon number, which includes ^{12}C and ^{13}C isotopes of each O_1 component.

The H/C ratios of saturate fractions computed from eq 1 were compared to those determined by the elemental analysis.

RESULTS AND DISCUSSION

Carbon Number Distribution of Saturates. The HT-GC chromatograms of the VR-derived saturate fractions are shown in Figure 1. The carbon numbers shown at the top of Figure 1 were based on the retention times of model *n*-paraffins. The results showed that the carbon number of *n*-paraffins in saturate fractions varied up to 100, except for SS, which was greater than 100. Because isoparaffins have lower boiling point temperatures than their corresponding normal isomers, the upper limit of the carbon number of isoparaffins should be greater than that of *n*-paraffins. The unresolved humps of chromatograms indicated that the composition of saturates was complex and HT-GC was inadequate to separate each compounds. The boiling point

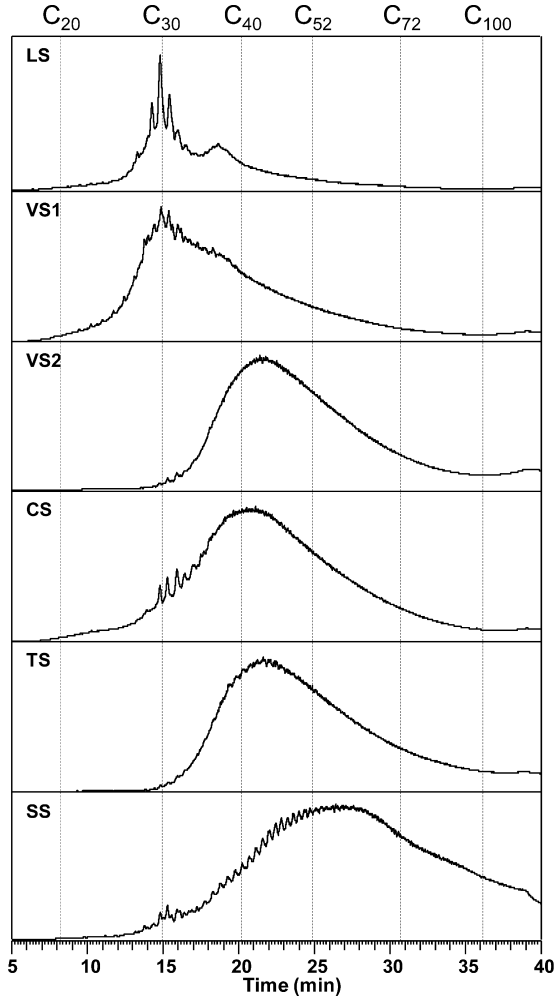

Figure 1. HT-GC chromatogram of saturates. The carbon numbers of the *n*-parrafins were marked above the chromatogram based on the retention times of the model *n*-parrafins.

curves for VR-derived saturate fractions are shown in Figure 2. The saturate fractions can be divided into two groups based on their initial boiling point. The LS and VS1 fractions were distilled at 420 °C, whereas the rest (VS2, CS, TS, and SS) was distillated at 500 °C. Apart from VS2 and TS, which overlapped

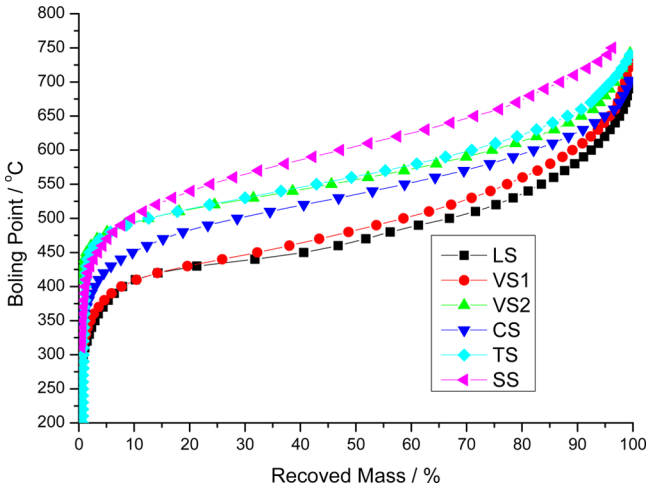

Figure 2. Simulated distillation curve of saturates.

each other, the chromatogram and distillation curve profiles for the saturate samples were distinct. For the LS, the bimodal distribution and sharp peaks of the chromatogram indicated that LS had a discontinuous distribution in its chemical composition. The tiny peaks for SS indicated the presence of large molecular *n*-paraffins.

Figure 3 shows the FT-ICR MS broadband spectra of saturate-derived RICO products before and after reduction by $LiAlH_4$. All of the abundant peaks corresponded to the O_1 class species. Figure 4 shows the distribution patterns of double bond equivalence (DBE) as a function of the carbon number of the O_1 class species in saturate-derived RICO products before and after reduction by $LiAlH_4$. The data in Figure 4 suggested that the naphthenes had higher maximum carbon numbers than the paraffins. This is expected because, at a given boiling point temperature, the carbon number of an isoparaffin or a naphthene is higher than that of a *n*-paraffin. The carbon number distribution determined by ESI FT-ICR MS was similar to that derived by HT-GC. However, the upper limit of the carbon number for each sample shown in Figure 4 was slightly lower than that determined by HT-GC. This is likely due to the mass discrimination and the relatively narrow detection dynamic range of FT-ICR MS.

The range of carbon numbers of the O_1 class species varied with the geological origin and distillation temperature of samples. The upper limit of the carbon number of the O_1 class species in CS, VS2, and TS was 85, and the upper limit of the carbon number of the O_1 class species in SS was 96. For 420 °C topped VR samples, the upper limit of the carbon number of the O_1 class species in VS1 was 75 and the upper limit of the carbon number of the O_1 class species in LS was 68. Because VS1 and VS2 were derived from the same crude oil, the different upper limits of the carbon number are likely ascribed to the detection dynamic range limitations of HT-GC and FT-ICR MS.

Naphthenes in Saturates. According to the mechanism of derivatization reactions,[20] the isoparaffins and naphthenes with tertiary C−H bonds are oxidized to tertiary alcohols. Normal paraffins and naphthenes without tertiary C−H bonds are selectively converted to form ketones in RICO oxidation reactions. The ketones can be reduced by $LiAlH_4$ reduction reactions to form alcohols. The mass spectra of RICO and RICO−$LiAlH_4$ reaction products show the presence of alkanes with tertiary C−H bonds and various types of alkanes, respectively. For example, the O_1 class species with 0 DBE in the saturate sample before and after $LiAlH_4$ reduction reactions were isoparaffins and paraffins (normal and iso), respectively. The O_1 class species in the saturate sample with DBE of *n* (where $n \geq 1$) corresponded to naphthenes with *n* rings.

The data presented in Figure 4 show that the relative abundances of various species in saturate samples were different depending upon the crude origins and distillation cut points. Naphthenes with 0−6 rings were relatively highly abundant. The upper limits of the DBE value for all saturate samples were similar, corresponding to a maximum number of naphthenic rings of 10. This value was much lower than some recent publications,[25,26] which indicated that the DBE value of saturates in crude oil could be more than 20, even up to 30. We prefer that the RICO results are more close to the real value, because a traditional open column separation method could not separate saturate and aromatic compounds completely; as a result, aromatic compounds with relatively low aromaticity are usually eluted into saturate fractions. The

dx.doi.org/10.1021/ef4016284 | *Energy Fuels* 2014, 28, 417−422

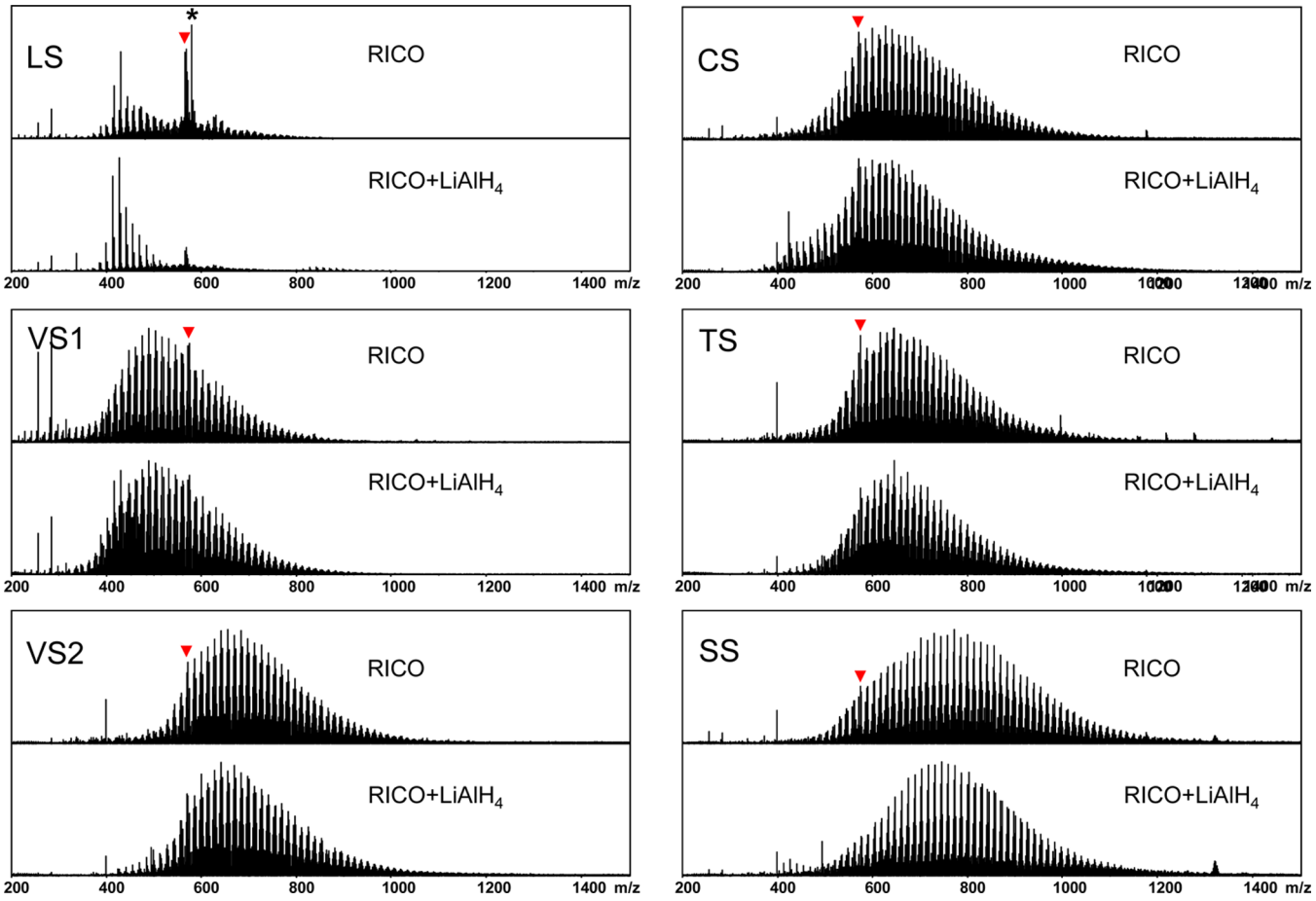

Figure 3. Broadband negative-ion ESI FT-ICR mass spectra of the O_1 species in the product of RICO and RICO−$LiAlH_4$ of saturates. The peaks marked with a red arrow are postulated as isoprenoid alkanes with a molecular formula of $C_{40}H_{80-2n}$ (n = 3−8). The peaks marked with an asterisk are likely contaminants.

RICO reactions preferentially oxidize co-eluted aromatic compounds in saturate fractions into carboxylic acids. This is critical for interpreting the MS data, because it is impossible to distinguish large molecular saturates from the bulk of heavy petroleum species without the co-elution of aromatic compounds with low molecular condensation by traditional separation methods.

According to our previous publication, the O_1 class species in RICO products are the major but not the exclusive products. For instance, squalane is oxidized to 20% ketones and 76% alcohols in a total yield of 53%, and cholestane is oxidized to 58% ketones and 24% alcohols in a total yield of 39%. The yield of oxidized products on the hydrocarbon is between 5 and 91%. The large variability of the yield implies that RICO could not be used as a quantitative approach for all of the saturate hydrocarbon analyses. However, the carbon number and DBE distribution obtained from RICO seem very similar to those from gas chromatography−field ionization mass spectrometry (GC−FIMS) for diesel saturates.[20]

To validate the results of carbon numbers and naphthenic rings, the H/C ratios of saturates calculated from MS analyses using eq 1 were compared to those from the elemental analysis, as shown in Table 1. The quantitative data from FT-ICR MS are just a single measurement. The H/C ratios of a Dagang saturate fraction (DS)[27] was also included for comparison. The data in Table 1 show that the H/C ratios calculated from MS analysis were consistent and slightly lower than those from elemental analysis. This can be due to the fact that alkanes with high DBE values have more tertiary C−H bonds and higher RICO reactivities compared to those with low DBE values, resulting in high abundance of MS peak intensity. From this point of view, the carbon numbers and naphthenic rings for saturate compounds in petroleum are likely reasonable, because the bias is toward high DBE alkanes in MS analysis. However, FT-ICR MS has a limited detection dynamic range; the results represent the major components found in the saturates and do not imply that compounds with more than 10 naphthenic rings are not present in heavy petroleum.

Even though RICO/ESI FT-ICR MS is not a proven quantitative analysis, the consistent and slightly lower H/C ratios from MS analysis showed that the method can be a potential quantitative analysis for heavy saturates. As shown in a previous paper,[20] RICO chemical derivatization followed by ESI FT-ICR MS was used to analyze saturates in heavy petroleum fractions. A series of model saturate compounds were used, and the results showed the formation of ketones and alcohols from RICO reactions of saturates. In addition, diols and hydroxy ketones can also form. However, because the selectivities of various products varied with reaction conversion, the product yields determined by MS analysis may not reflect the actual composition of saturates in the feed. Nevertheless, the results for diesel saturates were comparable to that from GC−FIMS.[20] This indicates the RICO/ESI and FI have similar selectivities for saturate compounds with various molecular

dx.doi.org/10.1021/ef4016284 | *Energy Fuels* 2014, 28, 417−422

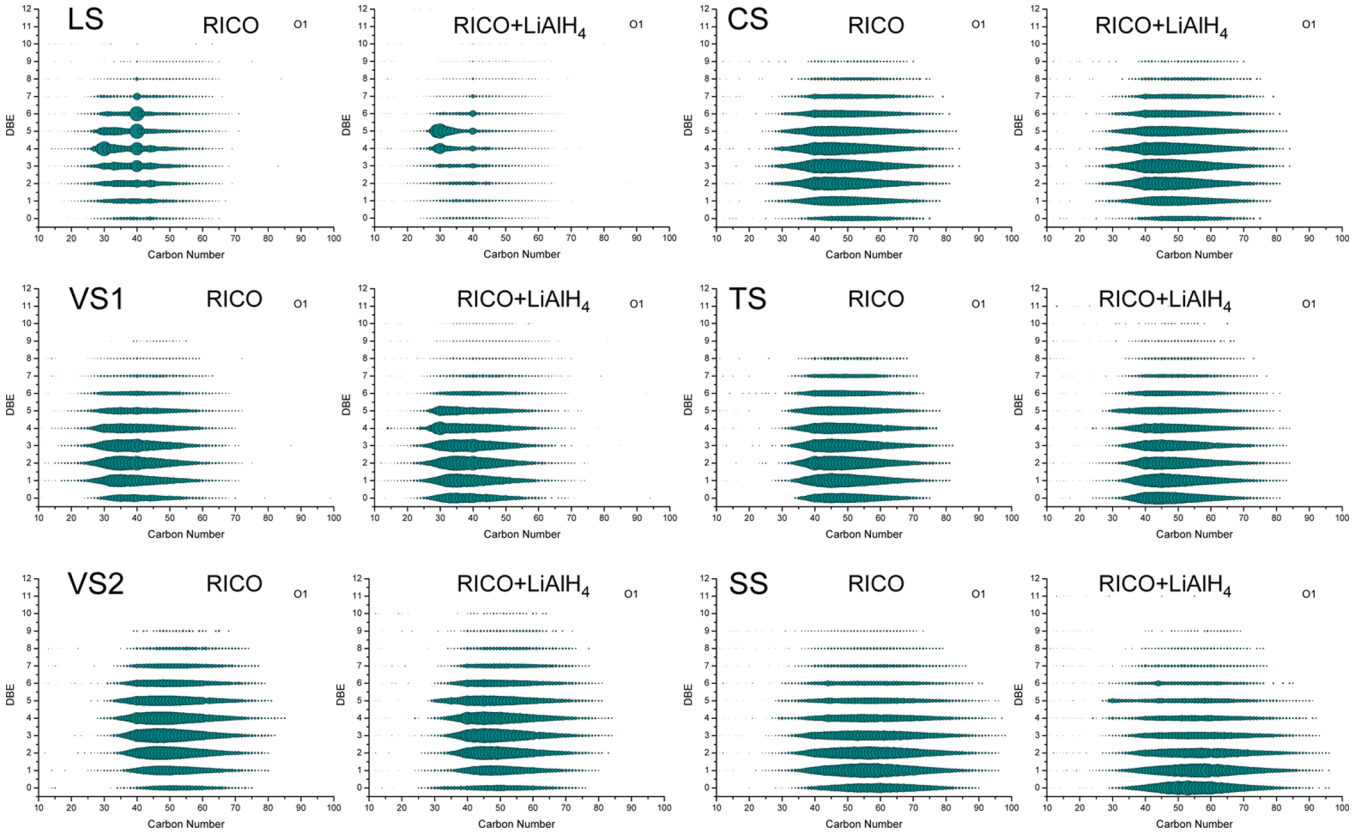

Figure 4. Isoabundance plots of DBE as a function of the carbon number for the O_1 class species from the negative-ion ESI FT-ICR MS of the product of (left) RICO and (right) RICO−$LiAlH_4$ reduction of saturates.

Table 1. Comparison of H/C Ratios of Saturate Fractions Obtained from Elemental Analysis (EA) and Mass Spectroscopy (MS)

ID	sample	origin	weight percent of residue (wt %)	H/C ratio by EA	H/C ratio by MS
1	SS	Sudan	17.50	2.12	1.97
2	DS[a]	Dagang, China	24.70	2.10	1.96
3	TS	Tahe, China	13.56	2.07	1.94
4	VS1	Venezuela	21.18	2.05	1.92
5	CS	Athabasca, Canada	8.27	2.02	1.90
6	VS2	Venezuela	7.30	2.01	1.91
7	LS	Liaohe, China	18.06	1.96	1.82

[a]Data were obtained from ref 27.

structures. In other words, RICO/ESI is semi-quantitative. A previous study[20] also showed that most model compounds with large molecular weights have RICO oxidation yields between 35 and 50; this is not a very large diversity compared to the ionization selectivity difference between petroleum molecules for general ESI and APPI analyses. Another factor that should be considered is the structural diversity of saturate compounds. For heavy petroleum fractions, such as VR, one molecular formula generally corresponds to a huge number of isomers. The oxidation and ionization selectivities of various compounds could converge to set values when averaging so many isomers based on the molecular formula. In addition, because the technique for heavy saturate characterization is limited, the RICO/ESI FT-ICR MS method can be considered as an alternative.

Isoprenoid Alkanes. The abundant mass peaks of LS mass spectra, shown in Figure 3, also indicate the presence of compounds with molecular formulas of $C_{40}H_{80-2n}$ (n = 3−8). This series of compounds with 40 carbons are likely isoprenoid alkanes.[28−30] Generally, isoprenoid alkanes have relatively more tertiary C−H bonds with relatively high RICO reactivity,[20] resulting in a higher MS peak intensity for the unreduced products. After $LiAlH_4$ reduction, ketones derived from other saturate compounds (generally with or without fewer tertiary C−H bonds) converted to alcohols, resulting in the decrease in relative abundance of MS peaks, because the "isoprenoid alkane" peaks are also abundant in the product after reduction by $LiAlH_4$. The C_{40} saturates were quite abundant compared to the adjacent species. Similar findings were also observed in other saturate samples; however, the relative mass peak intensities were less obvious. Compounds in LS with DBE of 4−5 and carbon numbers of 29−30 are likely steranes and hopanes. These compounds were abundant in the crude oils obtained from Bohai basin.[31]

CONCLUSION

The VR-derived saturates consisted of *n*-paraffins, isoparaffins, and naphthenes with 1−10 rings. The maximum DBE values of species in the VR-derived saturates were similar. The maximum carbon number of VR-derived saturates was almost 100, with maximum carbon number of CS, VS2, and TS being 85, SS being 96, VS1 being 75, and LS being 68. The maximum carbon numbers of naphthenes in VR-derived saturates were greater than those of paraffins. The relative abundances and

dx.doi.org/10.1021/ef4016284 | Energy Fuels 2014, 28, 417−422

ranges of carbon numbers of the various species in VR-derived saturates differed depending upon their geological origin and the distillation temperature of samples. Compounds with 0−6 naphthenic rings were highly abundant in the VR-derived saturates. On the bais s of the results of this study, the RICO/ESI FT-ICR MS method shows promise as a potential semi-quantitative analysis for saturates in heavy petroleum fractions.

AUTHOR INFORMATION

Corresponding Author

*Telephone: +86-10-8973-3738. E-mail: sq@cup.edu.cn.

Notes

The authors declare no competing financial interest.

ACKNOWLEDGMENTS

The authors thank Peidong Wang and Yongmei Liang for assisting with the GC analysis. This work was supported by the National Basic Research Program of China (2010CB226901) and the Fund of the National Natural Science Foundation of China (NSFC) (U1162204 and 21236009).

REFERENCES

(1) Strausz, O. P.; Morales-Izquierdo, A.; Kazmi, N.; Montgomery, D. S.; Payzant, J. D.; Safarik, I.; Murgich, J. *Energy Fuels* **2010**, *24* (9), 5053−5072.

(2) Qian, K. N.; Dechert, G. J. *Anal. Chem.* **2002**, *74* (16), 3977−3983.

(3) Briker, Y.; Ring, Z.; Iacchelli, A.; McLean, N.; Fairbridge, C.; Malhotra, R.; Coggiola, M. A.; Young, S. E. *Energy Fuels* **2001**, *15* (4), 996−1002.

(4) Schaub, T. M.; Hendrickson, C. L.; Quinn, J. P.; Rodgers, R. P.; Marshall, A. G. *Anal. Chem.* **2005**, *77* (5), 1317−1324.

(5) Smith, D. F.; Schaub, T. M.; Rodgers, R. P.; Hendrickson, C. L.; Marshall, A. G. *Anal. Chem.* **2008**, *80* (19), 7379−7382.

(6) Wu, C.; Qian, K.; Nefliu, M.; Cooks, R. G. *J. Am. Soc. Mass Spectrom.* **2010**, *21* (2), 261−267.

(7) Gao, J.; Owen, B.; Borton, D.; Jin, Z.; Kenttämaa, H. *J. Am. Soc. Mass Spectrom.* **2012**, *23* (5), 816−822.

(8) Dutta, T. K.; Harayama, S. *Anal. Chem.* **2001**, *73* (5), 864−869.

(9) Byrd, H. C. M.; Guttman, C. M.; Ridge, D. P. *J. Am. Soc. Mass Spectrom.* **2003**, *14* (1), 51−57.

(10) Kuhn, G.; Weidner, S.; Just, U.; Hohner, G. *J. Chromatogr., A* **1996**, *732* (1), 111−117.

(11) Kahr, M. S.; Wilkins, C. L. *J. Am. Soc. Mass Spectrom.* **1993**, *4* (6), 453−460.

(12) Chen, R.; Yalcin, T.; Wallace, W. E.; Guttman, C. M.; Li, L. *J. Am. Soc. Mass Spectrom.* **2001**, *12* (11), 1186−1192.

(13) Yalcin, T.; Wallace, W. E.; Guttman, C. M.; Li, L. *Anal. Chem.* **2002**, *74* (18), 4750−4756.

(14) Hanton, S. D. *Chem. Rev.* **2001**, *101* (2), 527−570.

(15) Campbell, J. L.; Crawford, K. E.; Kenttamaa, H. I. *Anal. Chem.* **2004**, *76* (4), 959−963.

(16) Crawford, K. E.; Campbell, J. L.; Fiddler, M. N.; Duan, P.; Qian, K.; Gorbaty, M. L.; Kenttämaa, H. I. *Anal. Chem.* **2005**, *77* (24), 7916−7923.

(17) Duan, P.; Fu, M.; Pinkston, D. S.; Habicht, S. C.; Kenttämaa, H. I. *J. Am. Chem. Soc.* **2007**, *129* (30), 9266−9267.

(18) Duan, P.; Qian, K.; Habicht, S. C.; Pinkston, D. S.; Fu, M.; Kenttamaa, H. I. *Anal. Chem.* **2008**, *80* (6), 1847−1853.

(19) Nyadong, L.; Quinn, J. P.; Hsu, C. S.; Hendrickson, C. L.; Rodgers, R. P.; Marshall, A. G. *Anal. Chem.* **2012**, *84* (16), 7131−7137.

(20) Zhou, X.; Shi, Q.; Zhang, Y.; Zhao, S.; Zhang, R.; Chung, K. H.; Xu, C. *Anal. Chem.* **2012**, *84* (7), 3192−3199.

(21) Ramljak, Z.; Solc, A.; Arpino, P.; Schmitter, J. M.; Guiochon, G. *Anal. Chem.* **1977**, *49* (8), 1222−1225.

(22) Shi, Q.; Dong, Z.; Zhang, Y.; Zhao, S.; Xu, C. *Chin. J. Instrum. Anal.* **2008**, *27* (S1), 246−248.

(23) Shi, Q.; Xu, C.; Zhao, S.; Chung, K. H.; Zhang, Y.; Gao, W. *Energy Fuels* **2009**, *24* (1), 563−569.

(24) Shi, Q.; Pan, N.; Long, H.; Cui, D.; Guo, X.; Long, Y.; Chung, K. H.; Zhao, S.; Xu, C.; Hsu, C. S. *Energy Fuels* **2013**, *27* (1), 108−117.

(25) Islam, A.; Cho, Y.; Yim, U. H.; Shim, W. J.; Kim, Y. H.; Kim, S. *J. Hazard. Mater.* **2013**, *263* (Part 2), 404−411.

(26) Gaspar, A.; Zellermann, E.; Lababidi, S.; Reece, J.; Schrader, W. *Energy Fuels* **2012**, *26* (6), 3481−3487.

(27) Zhou, X.; Shi, Q.; Zhang, Y.; Zhao, S.; Zhang, R.; Chung, K. H.; Xu, C. *Anal. Chem.* **2012**, *84* (7), 3192−3199.

(28) Kumar, S.; Agrawal, K. M.; Fischer, P. *Energy Fuels* **2004**, *18* (5), 1588−1594.

(29) Moldowan, J. M.; Seifert, W. K. *Science* **1979**, *204* (4389), 169−171.

(30) Albaigés, J.; Borbón, J.; Salagre, P. *Tetrahedron Lett.* **1978**, *19* (6), 595−598.

(31) Liao, Y.; Shi, Q.; Hsu, C. S.; Pan, Y.; Zhang, Y. *Org. Geochem.* **2012**, *47*, 51−65.